Triaxial Nuclei

G. Hagemann

2. Triaxial nuclei*

2.1. Introduction

Nuclei may acquire shapes with non-axial symmetry, but triaxiality is in general difficult to prove experimentally. Although signature effects are expected in energies as well as in electromagnetic properties, such effects may also arise as a result of the interplay of mechanisms not related to triaxiality. Unique, but substantially different effects of stable triaxiality are chiral twin bands and the wobbling mode.

The chiral symmetry relates to the orientation of the angular momentum vector relative to the three different intrinsic principal axes of the nucleus, and requires an orientation at variance with any of these. In such cases two solutions, with left- and right-handed orientation, respectively, may exist [57] leading to chiral twin bands. The wobbling mode, predicted more than 25 years ago [18] is uniquely related to a stable triaxial deformation, exploiting the rotational degree of freedom in a triaxial quantal system. For a triaxial body with different moments of inertia $\Im_i$ with respect to the principal axes (i.e. $\Im_x \gg \Im_y , \Im_z$) and in the high spin limit with most of the spin aligned along the x-axis, the wobbling mode introduces a sequence of bands with increasing number of wobbling quanta (n_w = 0,1,2, …) and a competition between the inter-band and the in-band transitions.

Most of the efforts at EUROBALL to study triaxiality has gone into the investigation of nuclei with strongly deformed triaxial shapes, and, as a break through, provided the first evidence for the wobbling mode [58,59]. Consequently, the focus of this section will be concentrated in this area. In a recent EUROBALL experiment the wobbling mode was even developed to the 2nd phonon excitation [60]. The wobbling interpretation is based on comparison to particle-rotor calculations [61]. In parallel with the experiments carried out at EUROBALL data have also been obtained from the GAMMASPHERE and GASP arrays. A discussion of these data will be included in the present status report on strongly deformed triaxial nuclei.

Nuclei with *N~94* and *Z~71* constitute a new region of exotic shapes coexisting with normal prolate deformation [62,63]. They provide a unique possibility of studying strongly deformed shapes with a pronounced triaxiality. At the beginning of the first EUROBALL campaign at Legnaro two such cases were known in ^{163,165}Lu [64-66]. Large Q_t values, corresponding to $\varepsilon \sim 0.4$ with $\gamma \sim 18°$, were derived for the triaxial superdeformed (TSD) band in ^{163}Lu [65] from both Recoil Distance and Doppler Shift Attenuation Method measurements. This band was interpreted as most likely corresponding to the $\pi i_{13/2}$ configuration. Later, a band with transition energies, identical within 1-3 keV to those in ^{163}Lu, was found in ^{165}Lu, and, based on the similarity, also interpreted as a $\pi i_{13/2}$ excitation. Calculations with the Ultimate Cranker (UC) code [67,68] based on a modified harmonic oscillator potential have revealed that large deformation minima are actually expected for all combinations of parity, π, and signature, α, in a region of nuclei around ^{163,165}Lu [64,69]. As an example a potential energy surface for ^{163}Lu is shown in Figure 2.1.

The most favourable even-even nuclei in the region among Yb-, Hf- and W-isotopes for finding low-lying TSD structures are calculated [68,69] to be ^{164,166}Hf. It appears that in spite of various searches no examples of TSD band structures could be found in those isotopes,

* Contribution by G. Hagemann

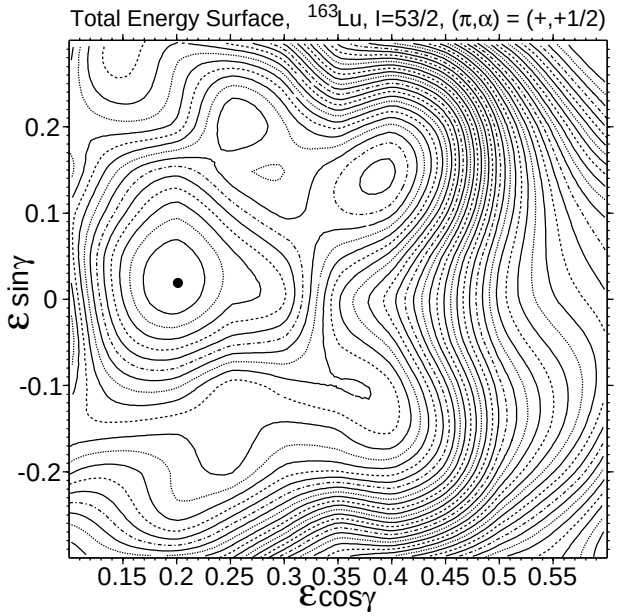

Figure 2.1: *Potential energy surface for ^{163}Lu and for parity and signature (π,α) = (+,+½) at spin I=53/2ħ; besides the normal minimum at $\varepsilon \sim 0.2$ two triaxial minima are developing at $\varepsilon \approx 0.4$ and with $\gamma \approx \pm 20°$.*

whereas there is new experimental evidence for three weakly populated TSD bands in ^{168}Hf, for which lifetime measurements have confirmed the large deformation [70]. It will be interesting to extend the search for TSD bands in the region to heavier Hf isotopes as well as to neighbouring Lu-isotopes. Lifetime measurements will also be required to substantiate the expected large deformations.

In addition to these investigations in the Lu-Hf region a recent EUROBALL experiment has revealed that a band in ^{154}Er, formerly interpreted as being superdeformed, but with properties resembling those found for TSD bands in the Lu-Hf region, should be reinterpreted as a TSD band (cf. Section 1). The expected superdeformed band with larger dynamic moment of inertia, $\mathfrak{I}^{(2)}$, and weaker population, was also established in this EUROBALL experiment [20]. The presumed triaxial structure in ^{154}Er most likely also has an $i_{13/2}$ proton involved in its configuration.

In this report on triaxial nuclei we will first concentrate on TSD bands in the Lu-Hf region; Sections 2.2 and 2.3 contain an overview of experiments and results and a presentation of the information on the spectroscopy of strongly deformed triaxial nuclei obtained primarily from EUROBALL measurements. The recent evidence for the 1st and 2nd phonon wobbling excitation Lu isotopes will be presented in section 2.4. New results on chirality in nuclei will be discussed in section 2.5 followed by some conclusions and perspectives.

2.2. General properties of strongly deformed triaxial nuclei

Figure 2.2 shows an overview of TSD bands found in Lu- and Hf-nuclei in the recent years. These data have come from the EUROBALL, GAMMASPHERE and GASP arrays. The very first TSD band in the region, TSD1 in ^{163}Lu, with a population of ~10% relative to the yrast strength in the reaction channel, was found with the OSIRIS array (12 Ge-detectors with an inner BGO ball) [65]. Lifetimes for that band were later measured with the NORDBALL array consisting of 20 Ge detectors with a BGO INNER BALL of 55 elements [66].

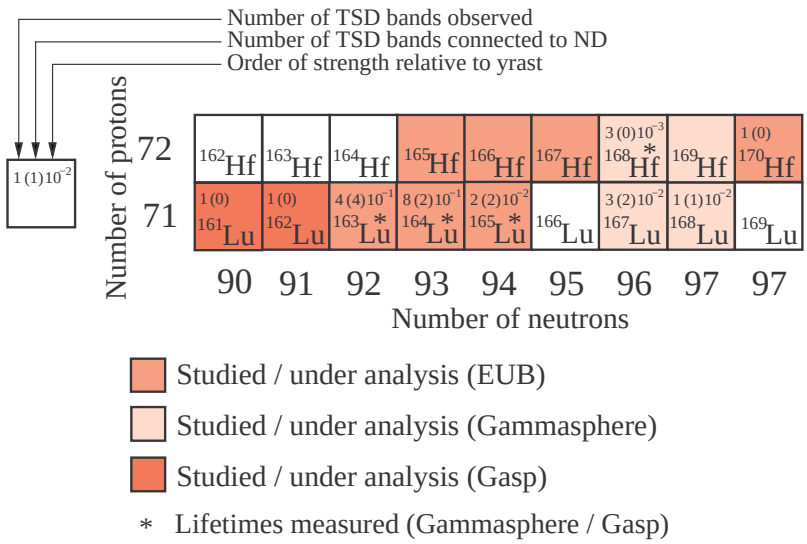

Figure 2.2: *Overview of searches and results for Lu and Hf nuclei. References for TSD band structures are: ^{161,162}Lu [71], ^{163}Lu [65,72,59], ^{164}Lu[73], ^{165}Lu [64,74], ^{167}Lu [75, 76], ^{168}Lu [77], ^{166}Hf [78], ^{168}Hf [70] and ^{170}Hf [79]. In addition, at the time of writing this report a new Euroball experiment with the aim of studying further the bands found in ^{161,162}Lu is being performed. References for lifetime measurements on TSD bands are: ^{163,164,165}Lu [66,80,81] and ^{168}Hf [70].*

It should be noted that the expected, most favourable nucleus for TSD structures, ^{164}Hf has been studied with NORDBALL, with negative results. Although NORDBALL was considerably less effective at discovering long cascades of γ-rays than the later arrays included in Figure 2.2, a TSD band of a strength comparable to those seen in ^{163}Lu and ^{165}Lu, should have shown up in the NORDBALL data. Furthermore, ^{165,166,167}Hf were studied with EUROBALL, but once again no TSD bands were found [78].

The identification of TSD bands in the Lu-Hf nuclei is in most cases based on the observation of large dynamic moments of inertia similar to the first observed TSD bands in ^{163}Lu and ^{165}Lu. A comparison of the values for odd-N and even-N Lu isotopes is shown in Figure 2.3.

For most of the bands quoted in Figure 2.2 it has not been possible to establish connections to known normal-deformed (ND) structures. Therefore, the excitation energy, spin and parity are unknown. However, with reasonable assumptions of alignments (comparable to what has been determined in ^{163,165}Lu and ^{164}Lu), the spins of the unconnected bands can be estimated within ~2$\hbar$. The relative population of the TSD bands compared to the yrast normal-deformed structures in the same nucleus must be related to the excitation energy of the local, triaxial

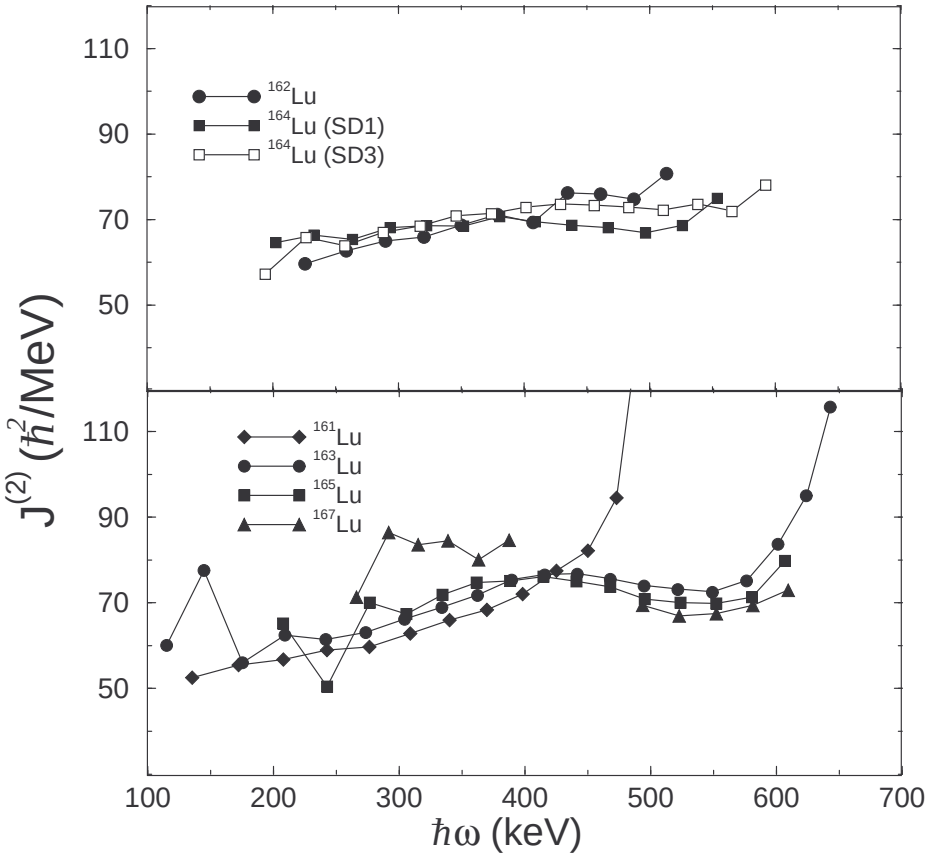

Figure 2.3: *Dynamic moments of inertia $\mathcal{J}^{(2)}$ for Lu isotopes with odd (top) and even neutron numbers (bottom). References for the individual nuclei are given in the caption to Figure 2.2.*

superdeformed minimum relative to the global normal defomed minimum in the potential energy surface (see Figure 2.1.). From such a comparison one can conclude that among the lighter Lu isotopes, ^{163}Lu has the lowest TSD minimum. The population strength found in ^{161,162}Lu is considerably lower than in ^{163}Lu. The strength found in ^{165}Lu seems to stay constant (or even increase) towards the heavier isotopes, ^{167,168}Lu. For the two even-even Hf isotopes an increase by a factor of ~3.5 is measured in the population of the new TSD band in ^{170}Hf over the population of the strongest TSD band in ^{168}Hf, to which the one in ^{170}Hf has a pronounced resemblance.

In conclusion, it seems that the pattern of population does not match what should be expected from the properties of the local triaxial minima calculated by the cranked shell model [68,69] for the even-even nuclei in the region.

2.3. New results on TSD bands in the Lu-Hf region

In the first very successful EUROBALL experiment on triaxial structures eight TSD bands were established in the odd-odd isotope ^{164}Lu. Connections to the normal-deformed structures were found for two of the strongest populated TSD bands. In the same experiment the complete decay-out from the first TSD1 band in ^{163}Lu could be established, and the spin and parity assignment confirmed its interpretation as a $\pi\, i_{13/2}$ configuration. The two connected TSD bands in ^{164}Lu with firm spin and parity assignments could be interpreted as also based on an

$i_{13/2}$ proton, coupled to neutrons occupying the lowest positive and negative parity orbitals, respectively [73].

Partial level schemes of ^{164}Lu [73] and ^{163}Lu [60,72] are shown in Figures 2.4 and 2.5, respectively. These two nuclei represent the most comprehensive determination of different decay-out properties of states in a TSD well to the normal-deformed structures. The mechanism behind the decay-out from a potential well of a different shape to the normal-deformed well (cf. Section 3) will depend on its excitation energy and on the height of the barrier between the two minima.

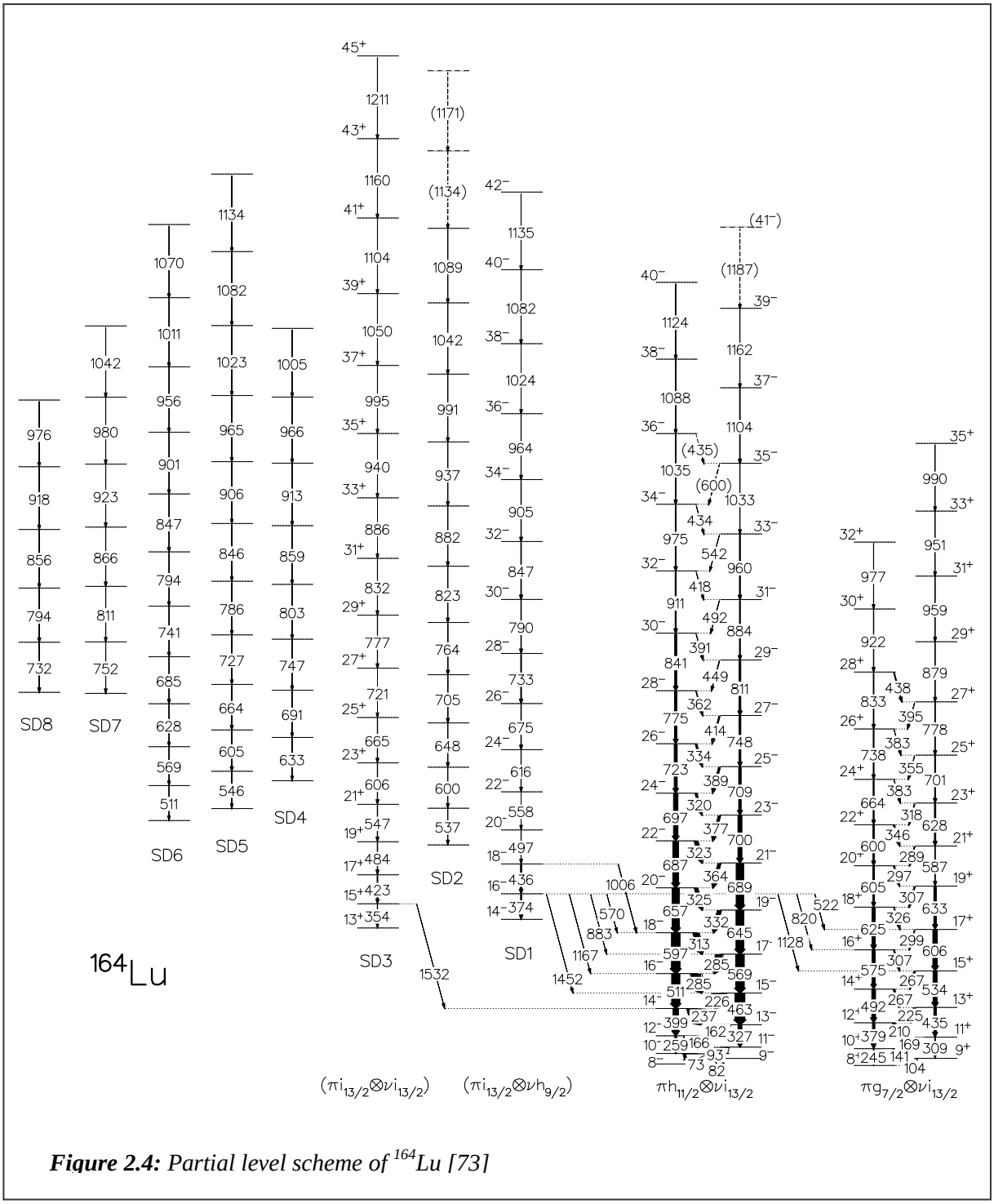

Figure 2.4: *Partial level scheme of ^{164}Lu [73]*

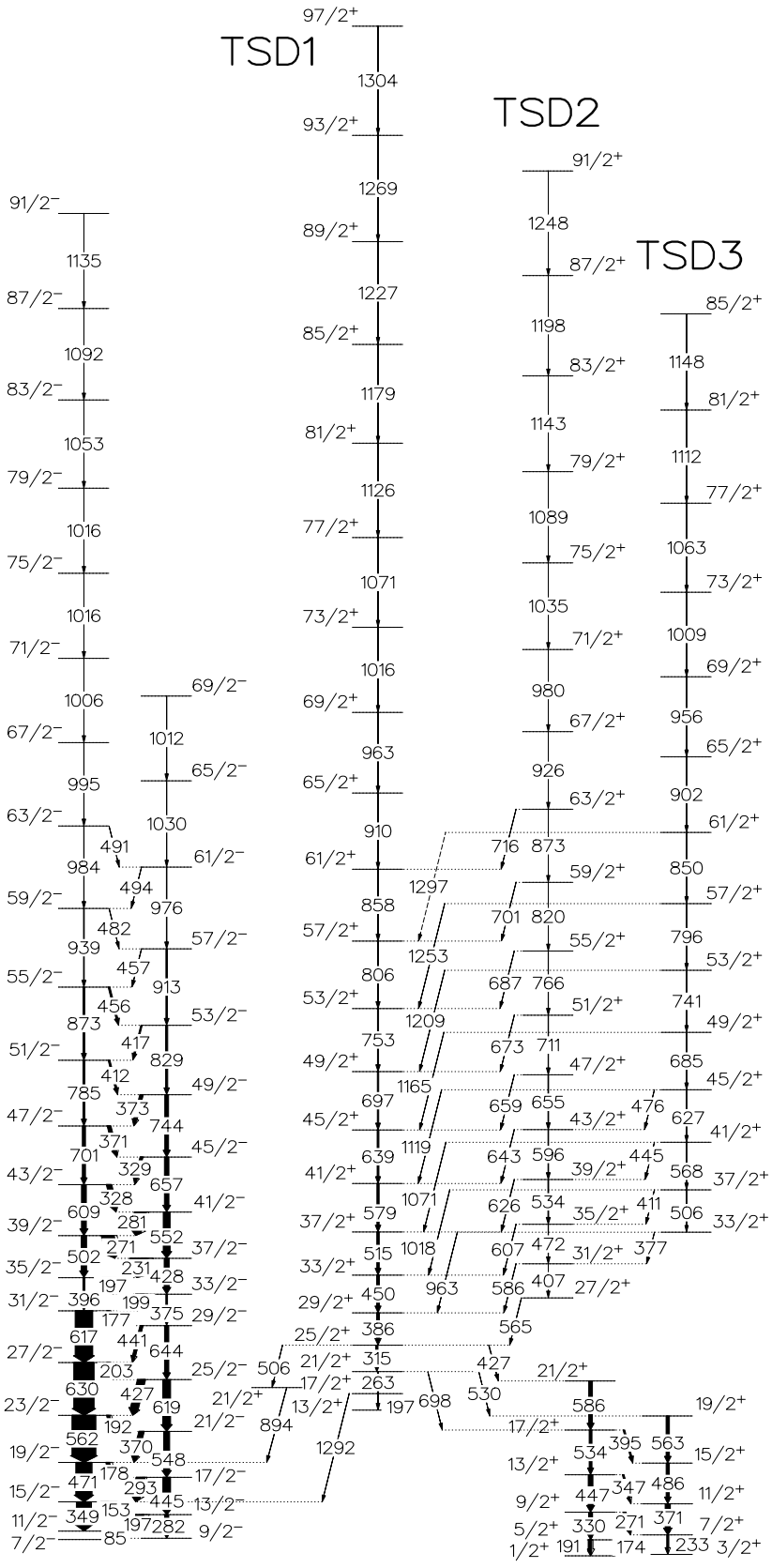

Figure 2.5: *Partial level scheme of ^{163}Lu showing the three TSD bands together with the connecting transitions to the ND-structures to which the TSD states decay [72,60].*

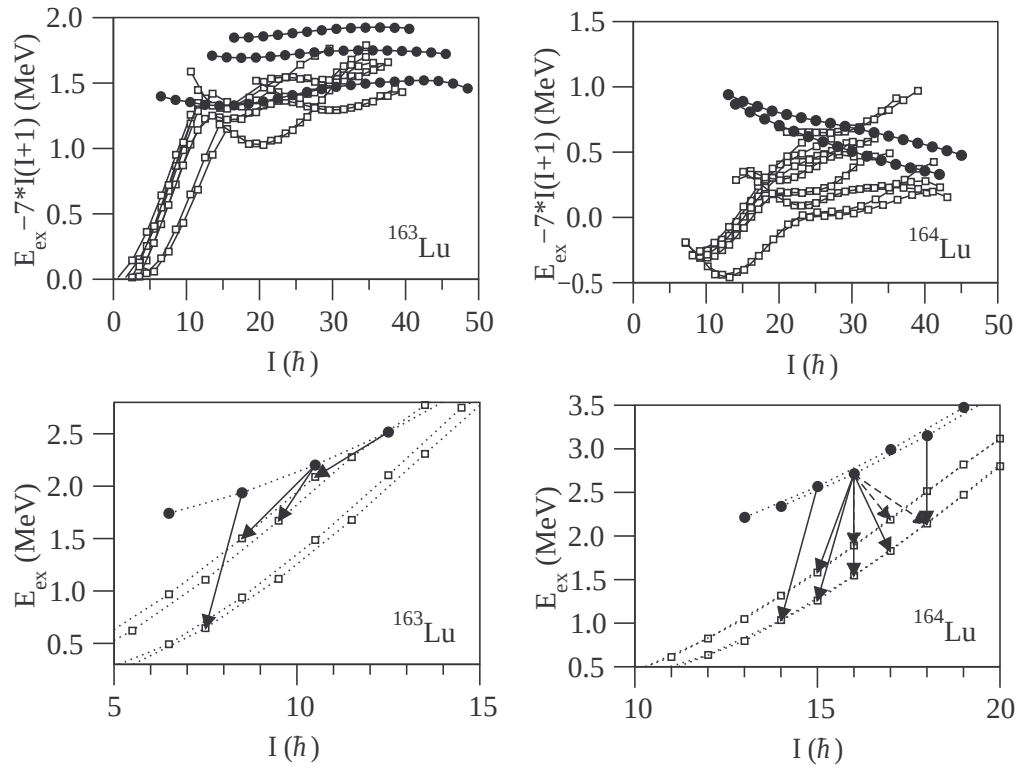

Figure 2.6 (Top panels): *Excitation energy relative to a rigid-rotor reference of the TSD bands (filled circles) together with normal-deformed bands (open squares) in ^{163}Lu and ^{164}Lu.* ***(Bottom panels):*** *Excitation energy in the spin region where the decay-out of the TSD bands takes place for ^{163}Lu and ^{164}Lu. Only bands in connection with the TSD band decay are shown. The arrows represent the observed connecting transitions. The figure is taken from Ref. [82].*

Two different decay-out scenarios are demonstrated in Figure 2.6 [82]. The preferred decay of a particular TSD band will depend on the excitation energy, relative to normal-deformed structures with the potential of causing a mixing of the TSD and normal-deformed states at their closest distance, at the lowest spins. The decay-out observed in ^{164}Lu of TSD1 with (π,α) = (-,0) shown in the bottom-right part of Figure 2.6, comprises both stretched and unstretched E1 and E2 transitions, the strongest decay being the stretched $16^- \rightarrow 15^+$ E1-transition. For TSD3 with (π,α) = (+,1) only one stretched E1 transition was found. From the out-of-band to in-band branching ratios the strongest E1 decay-out transitions are estimated to be of the order of $\sim 0.3 \cdot 10^{-4}$ W.u., which is around 300 times faster than the E1 decay found for the (axially symmetric) superdeformed states in ^{194}Hg [25], and only ~5 times slower than octupole-enhanced E1 transitions between some of the normal-deformed structures in the same and neighbouring nuclei. This suggests that octupole enhancement may also play a role in the TSD to ND E1 decay. From a similar consideration the B(E2, TSD $\rightarrow$ ND) values are 10^3 - 10^4 times reduced compared to the TSD in-band B(E2)-values.

In contrast, the decay-out from TSD1 in ^{163}Lu at spins I = 23/2 and 21/2 $\hbar$ can be completely explained by mixing at spin I = 21/2 $\hbar$, with a rather large interaction strength (~22 keV). Since the band TSD1 comes considerably closer to the normal-deformed structures at higher spin with no observation of cross-band transitions one may conclude that the barrier separating the two minima is probably more efficient at higher spin values, which also agrees with calculations. The different branching ratios also contain information on the ratio of the

quadrupole moments, i.e. $Q_t(TSD)/Q_t(ND) \sim 2$, which confirms the larger deformation of TSD1. The weak E1 decay observed from the $17/2^+$ state resembles the E1-decays observed in ^{164}Lu.

In addition to the decay out properties of ^{163,164}Lu summarised in Figure 2.6, there are data from GAMMASPHERE under analysis on the decay-out in ^{167,168}Lu [76,77], and a very recent EUROBALL experiment has provided new data on ^{165}Lu [74]. In both of these even-N Lu-isotopes the decay-out of the yrast TSD band occurs through mixing with normal-deformed states as in ^{163}Lu, however in ^{167}Lu the TSD and normal-deformed bands cross and interact at intermediate as well as at low spin.

2.4. The wobbling mode and the first and second phonon excitation

The most striking feature of the level scheme of ^{163}Lu shown in Figure 2.5 is that all decays of the excited TSD bands proceed through the yrast TSD1 band. In addition, all three bands have very similar dynamic moments of inertia and alignments over almost the entire observed frequency range. The multipolarity of the transitions from TSD2 and TSD3 to TSD1 and from TSD3 to TSD2 have been determined by the analysis of the Directional Correlation from Oriented states, angular distribution ratios and linear polarisation data of the strongest transitions. It has thereby been possible to assign firm spins and positive parity to this family of bands, and a pattern compatible with expectations from wobbling phonon excitations has emerged [58-61].

The wobbling degree of freedom in an odd, triaxial nucleus like ^{163}Lu with aligned particle angular momentum in addition to the collective angular momentum is different from the original picture presented for an even-even system [18]. Here the total angular momentum is tilted away from the axis of the largest moment of inertia by a “wobbling angle”, which

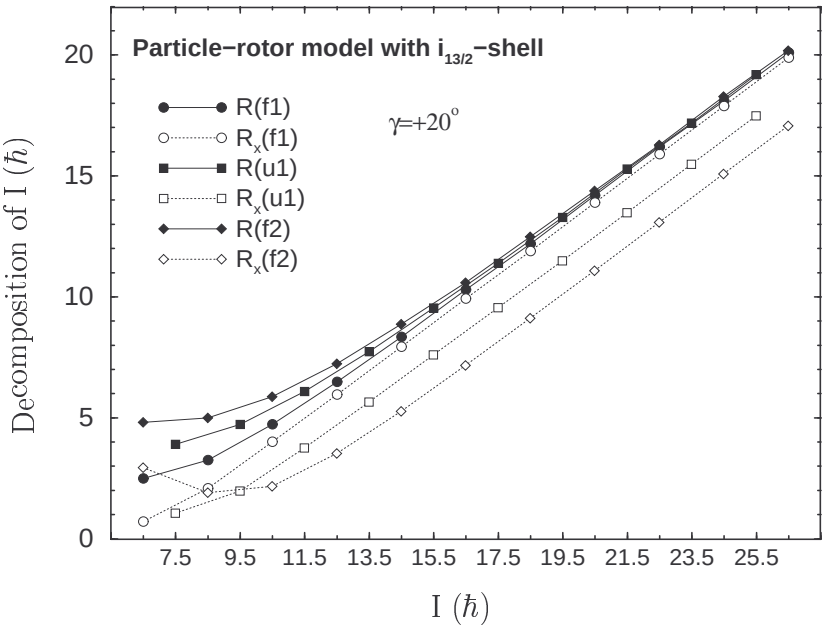

Figure 2.7: *Calculated expectation values of the collective angular momentum and its projection on the x-axis for the lowest favoured (f1, f2) and unfavoured (u1) bands in ^{163}Lu; f1, u1 and f2 correspond to bands with n_w = 0, 1 and 2, respectively[61].*

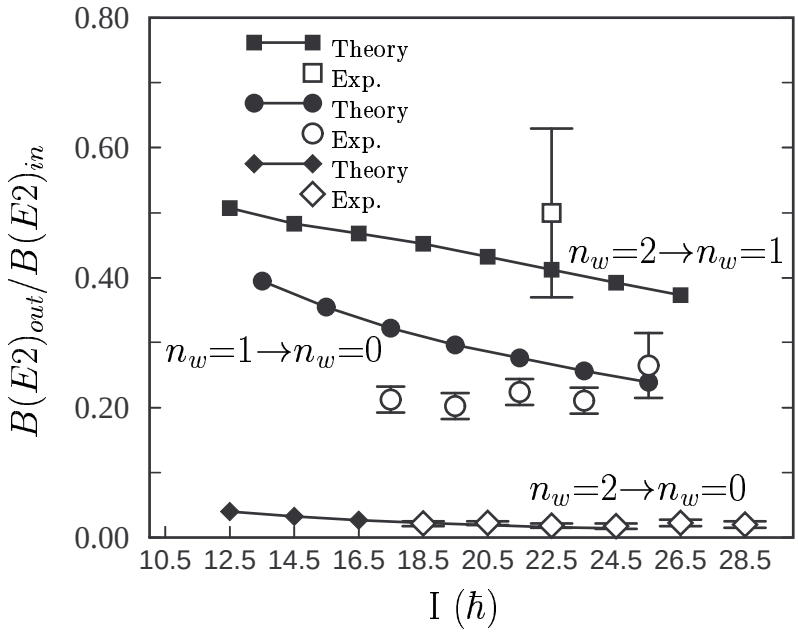

Figure 2.8: *Experimental and theoretical values of $B(E2)_{out}/B(E2)_{in}$. TSD1, TSD2 and TSD3 are identified with n_w = 0,1 and 2, respectively [60].*

increases with the phonon number n_w. The possible presence of the angular momentum coming from intrinsic motion can in many ways make the nuclear wobbling mode much richer. The presence of aligned particles favours a particular (triaxial) shape and produces a unique pattern of electromagnetic transitions between the bands. The decomposition of the collective angular momentum shown in Figure 2.7 has been calculated with a model in which the aligned particle is coupled to a triaxial rotor [61]. The lowest solution with positive parity and favoured signature (α=+½), *f1*, has the collective angular momentum fully aligned with the x-axis (of largest moment of inertia). This solution is identified with TSD1 in ^{163}Lu. The second lowest solutions, *f2*, obtained with (π,α)= (+,+½) has a considerably smaller expectation value of the component R_x than *f1*. For the lowest solution with positive parity and unfavoured signature, (α=-½), *u1*, the expectation value of R_x is intermediate between *f1* and *f2*, thus bearing out the expected increase in wobbling angle, here for the collective part of the angular momentum.

The most crucial information from the particle-rotor calculations in Ref. [61] is contained in the electro-magnetic transition matrix elements. In particular, in the spin-range covered by the experiment the B(E2, $n_w = 1 \rightarrow n_w = 0$) values for the inter-band transitions are calculated to be around 22-30% of the collective in-band B(E2, $n_w = 1 \rightarrow n_w = 1$) values, which is large compared to single-particle values. Furthermore, with a wobbling phonon description it is expected that B(E2, $n_w = 2 \rightarrow n_w = 1$) ~ 2 · B(E2,$n_w = 1 \rightarrow n_w = 0$). The values of B(E2, $n_w = 2 \rightarrow n_w = 0$) are small and only nonzero due to anharmonicities in the quantal phonon description.

In Figure 2.8 the data obtained for ^{163}Lu are compared to calculations. The agreement illustrated in the figure, together with difficulties in alternative interpretations of the large B(E2) values for the TSD2 → TSD1 transitions and in particular the crucial TSD3 → TSD2 transition, provides the principal evidence for the wobbling excitation mode in ^{163}Lu with both the 1st and 2nd phonon modes being established. New data in ^{165,167}Lu [74,76] show

candidate bands with very similar properties to the TSD2 band, and for ^{165}Lu also the TSD3 band, in ^{163}Lu. In both nuclei the electromagnetic properties, when measurable, also resemble those found in ^{163}Lu. Very recent Euroball data on ^{161}Lu also indicate the existence of the 1st phonon wobbling excitation connected to the TSD band.

2.5. New Results on chirality in nuclei

The most likely candidates to show chiral twin bands are odd-odd triaxial nuclei in which the odd proton and neutron occupy orbitals with specific preference for two of the principal axes, while the collective rotation preferring the third axis ensures that the angular momentum is oriented out of any of the principal planes. Some cases are suggested in the region around ^{134}Pr [83,84], and data from a recent EUROBALL experiment may indicate the possibility for the existence of chiral twin bands in even-even ^{136}Nd, although the two candidate bands may also be interpreted differently [85]. Recently, experiments have been carried out on the odd-odd nuclei ^{130,132}Cs [86] using the EUROBALL IV array at Strasbourg. These are near-neighbours to ^{134}Pr, and potential chiral structures have been previously observed at low-spin in both nuclei [87]. The prime focus of the experiment on ^{130}Cs is to measure the lifetimes of the states and hence determine the in-band and inter-band B(E2), B(M1) transition rates. These data will be particularly important since B(M1)/B(E2) ratios deduced for the chiral bands in ^{134}Pr are proving to be difficult to understand in terms of the chiral picture.

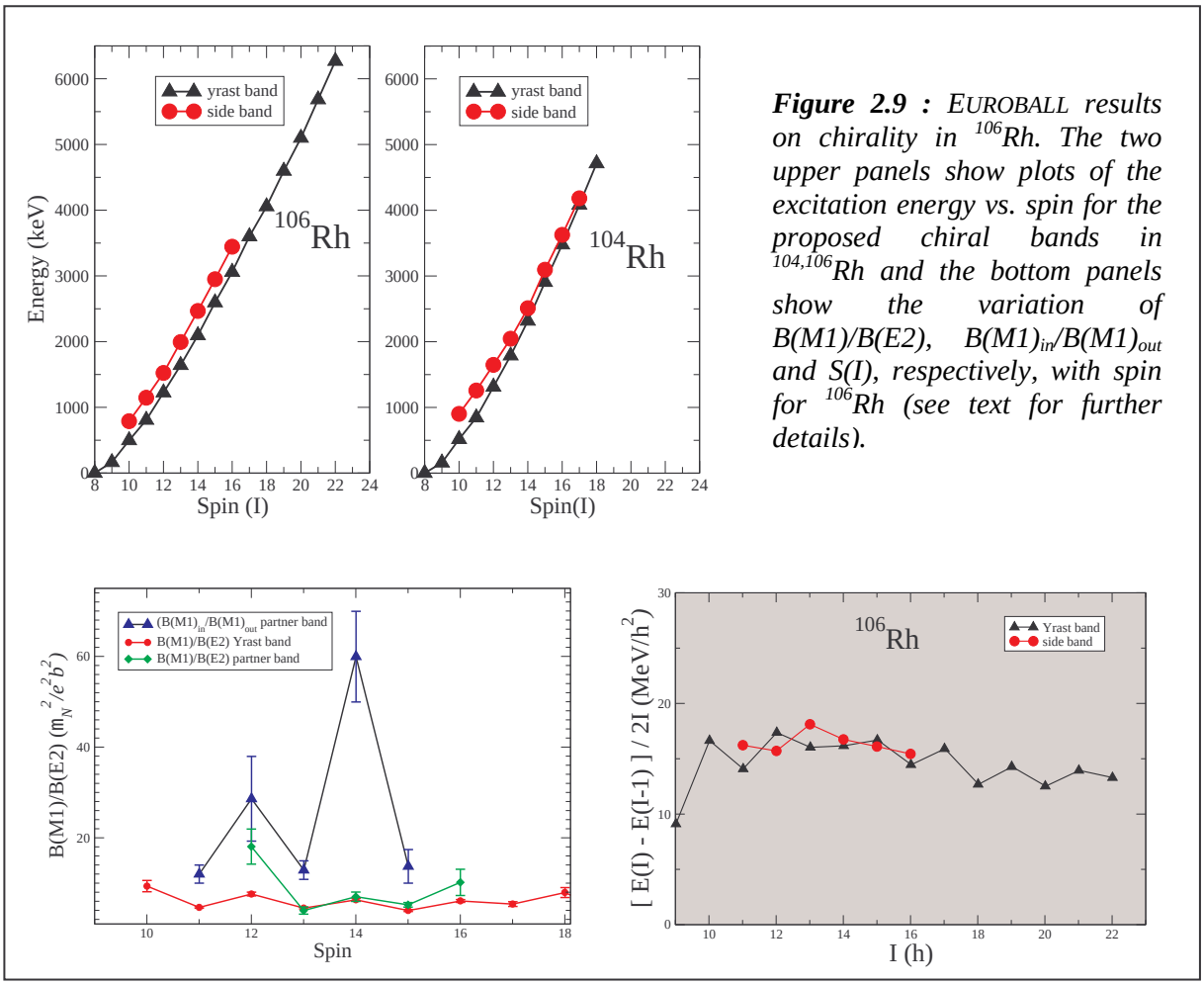

Figure 2.9 : *EUROBALL results on chirality in ^{106}Rh. The two upper panels show plots of the excitation energy vs. spin for the proposed chiral bands in ^{104,106}Rh and the bottom panels show the variation of B(M1)/B(E2), $B(M1)_{in}/B(M1)_{out}$ and S(I), respectively, with spin for ^{106}Rh (see text for further details).*

Recent studies have highlighted a new region of chiral structures in the neutron rich rhodium nuclei; the first case being identified in ^{104}Rh [88]. In this study the authors reported three fingerprints for the observation of chiral structures in nuclei. These may be summarised as follows: (1) the presence of near degenerate doublet $\Delta I=1$ bands over a range of spins; (2) the parameter $S(I) = [E(I) - E(I-1)] / 2I$ should be independent of spin and (3) there exists chiral symmetry restoration M1 and E2 selection rules as a function of spin. According to theoretical predictions the latter results in a staggering of the B(M1)/B(E2) ratios for in-band transitions and a similar staggering (with the same phase) for the ratio of the B(M1) in-band to B(M1) out of band transitions, $B(M1)_{in}/B(M1)_{out}$.

A recent experiment on neighbouring nuclei, carried out using EUROBALL, has revealed further evidence in support of this new region of chiral nuclei (see figure 2.9). The data for ^{106}Rh show good agreement with the above fingerprints, and consequently provides further evidence for the existence of chiral structures in this mass region. One clear difference between ^{106}Rh and ^{104}Rh, which can be seen in Figure 2.9, is that the chiral partner bands do not become degenerate in ^{106}Rh. Instead, they appear to have a near constant separation of ~350 keV. This is reminiscent of observations for nuclei neighbouring ^{134}Pr in the A=130 region, where the effect was attributed to the existence of chiral vibrations rather than chiral rotation [84]. The present experiment has also revealed the first evidence for chiral structures in an odd mass nucleus in this mass region, ^{105}Rh [89]. The properties of the observed structure suggest that this is the best example of chirality in an odd mass nucleus observed to date in any mass region.

2.6. Conclusions and perspectives

A new and very interesting region of nuclei presenting strongly deformed triaxial shapes has been revealed, by experiments carried out primarily with the EUROBALL array. Triaxiality provides the possibility of studying coexistence not only between different shapes, but also between the normal cranking solution in the strongly deformed triaxial well and the wobbling-phonon excitation, which represents a different manifestation of the rotational degree of freedom, that is realised in a triaxial nuclear quantal system.

Firm evidence for stable triaxiality is obtained from the presence of both the 1st and 2nd phonon wobbling excitations in ^{163}Lu. Wobbling excitations are present in the neighbouring nuclei ^{165,167}Lu and possibly also in ^{161}Lu, which confirms wobbling as a general phenomenon of triaxially deformed nuclei. It remains a challenge to establish a wobbling excitation in an even-even nucleus without having particle alignment in addition to the collective angular momentum. Other regions of nuclei may be found with a favourable potential for local triaxial minima as shown for example by the case of ^{154}Er [20] and possibly its neighbours (cf. Section 1).

Different decay-out mechanisms from a strongly deformed (local) triaxial minimum have been identified. The size of mixing matrix elements is related to the barrier between TSD and normal-deformed minima. Pure statistical decay-out is found when levels do not come sufficiently close to the normal-deformed states. The decay-out transitions of E1 character may be octupole enhanced. Further support for the coexistence of minima of different shapes comes from a fluctuation analysis of the number of bands in the different wells (cf. Section 4), showing that a large number of triaxial bands exist before damping of the rotational strength sets in [90].

The present variance between predictions from the cranked shell model and the experimental results concerning the most favourable location and relative excitation energy of the triaxial minima presents a challenge to nuclear structure theory. With spectroscopy in the triaxial well further developed a better understanding of the exact location of the shape-driving orbitals underlying the triaxial shapes can be obtained. In addition to the particle-rotor calculations, which provide the basis for our evidence for the observation of wobbling-phonon excitations, alternative theoretical formulations, for example using the cranked shell model plus random phase approximation [91] now exist. Other attempts from nuclear structure theory are underway.

Finally, there is also a growing body of evidence in support of the existence of the phenomenon of chirality in nuclei. At the present time the mass 130 region has received most attention, both theoretically and experimentally. Here there is evidence for chiral rotation in ^{134}Pr, with an island of odd-odd nuclei surrounding this nucleus, which have structures that have been interpreted in terms of chiral vibrations [83]. Chiral rotation may be expected to be found in nuclei which have a stable triaxial shape and valence protons and neutrons occupying high-j hole- and particle-like orbitals (or vice versa) respectively. Recent work suggests that nuclei in the Rh region around mass 100, where structures involving $g_{9/2}$ proton holes and $h_{11/2}$ neutron particles have been found, provide some of the best examples of chiral rotation and vibration observed to date. However, many other potential regions remain unexplored. It will be interesting to see if any of these can provide more than one example of chiral rotation, as seems to be the limit in the two regions explored so far.

Acknowledgements

The author is indebted to the large collaborations working on triaxiality and wobbling for help and communication of unpublished results, in particular to D.R. Jenssen, S.W. Ødegård, I. Hamamoto, P. Bringel, G. Schönwasser, A. Neußer, H. Amro, and to R. Wadsworth for the results on chirality.